ARMA 16-829

Shear Reactivation of Natural Fractures in Hydraulic Fracturing

Moradian, Z.
Earth Resources Laboratory (ERL), Massachusetts Institute of Technology (MIT), Cambridge, MA, 02139
Fathi, A.
Département de Génie Civil, Université de Sherbrooke, 2500 Boul. de l'université, Sherbrooke, Québec, Canada J1K 2R1
Evans, B.
Earth Resources Laboratory (ERL), Massachusetts Institute of Technology (MIT), Cambridge, MA, 02139

This paper was prepared for presentation at the 50th US Rock Mechanics / Geomechanics Symposium held in Houston, Texas, USA, 26-29 June 2016. This paper was selected for presentation at the symposium by an ARMA Technical Program Committee based on a technical and critical review of the paper by a minimum of two technical reviewers. The material, as presented, does not necessarily reflect any position of ARMA, its officers, or members. Electronic reproduction, distribution, or storage of any part of this paper for commercial purposes without the written consent of ARMA is prohibited. Permission to reproduce in print is restricted to an abstract of not more than 200 words; illustrations may not be copied. The abstract must contain conspicuous acknowledgement of where and by whom the paper was presented.

ABSTRACT: Fluid transport during hydraulic fracturing can be either proppant or asperity dominated. In the absence of proppants, dilatancy of the natural fractures during shear reactivation is required to provide sufficient aperture and hydraulic conductivity. If a hydraulic fracture intersects a natural fracture, the fracturing fluid enters the natural fractures, increasing pore pressure and decreasing the effective normal stress on the fracture plane. If the effective normal stress becomes low enough, the natural fracture may slip and dilate, resulting in increased aperture and hydraulic conductivity. To understand these processes, we conducted direct shear tests on rock fractures with constant normal load and examined the effect of slip and dilatancy of asperities on mechanical aperture. Using 3D coordinates of the surface asperities and measuring shear displacement and dilation during shear testing, the evolution of the mechanical aperture was calculated as a function of slip and normal stress. The calculation suggested that when effective normal stress is low, small slip events along a rough surface can induce dilatancy along the fracture surface that will cause considerable increases in the hydraulic aperture of the fracture.

1. INTRODUCTION

Proppants are introduced during hydraulic fracturing to increase fracture transmissivity during well production (Cipolla et al. 2009). But can fracture conductivity also be increased without proppant, for example, by water fracing? (Mayerhofer et al 1997). In contrast to conventional propped hydraulic fracture treatments, water fracs rely on reactivation of natural fractures to induce permanent shear induced dilation, which enhances reservoir permeability (Chen et al 2000, Weng et al 2015). Although the conductivity of un-propped shear-induced fractures is relatively low compared to that of the propped fractures, such conductivity can still play an important role in enhancing the productivity of ultra-low-permeability rocks like shale (Zhang et al. 2013, Weng et al 2015, Jansen et al. 2015).

Shear reactivation of natural fractures and fault planes in shale gas reservoirs is likely to be the main deformation mechanism during hydraulic fracturing stimulation (Zoback et al. 2012). During hydraulic fracturing, two mechanisms can cause shear reactivation of natural fractures; the first occurs when the elevated stresses around the tip of the propagating hydraulic fracture cause slip on the nearby natural fracture (Figure 1). This mechanism is governed by the stress, failure properties (cohesion and friction) of the fracture, and the orientation of the plane, in addition to the length of the hydraulic fracture (Maxwell et al 2015). If no fluid enters the natural fracture, the pore fluid pressure will remain unchanged. Thus slip occurs under high normal loads, damage will occur along the rough asperities and the net amount of dilation will be reduced. Transmissivity along the fracture may increase only a small amount or perhaps even decrease.

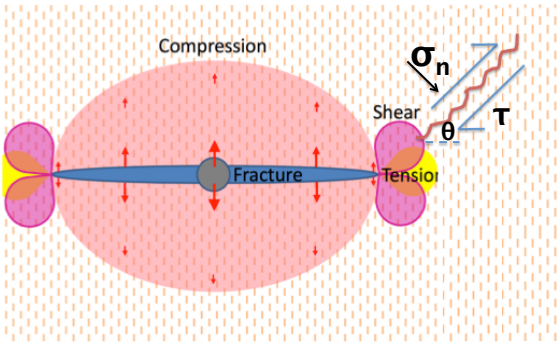

Fig. 1. Shear reactivation of natural fracture caused by shear stress at the tip of the hydraulic fracture (modified from Maxwell et al. 2015). It is assumed that the hydraulic fracture doesn't intersect the natural fracture and that the matrix is impermeable. Due to high damage and gouge production, this mechanism may not create considerable aperture and hydraulic conductivity.

For the second mechanism (Figure 2), the hydraulic fracture intersects the natural fracture and if the natural fracture is permeable enough, fracturing fluid can enter, increasing pore pressure and decreasing the effective normal stress and, perhaps, making it become tensile (Maxwell et al 2015). The slip along the rough surface that results can cause increases in aperture and hydraulic conductivity. In this mechanism since effective normal stress is low, less damage will occur and gouge production will be small. After reactivation of the natural fracture, even when pumping ceases and the normal load along the fault is positive, the hydraulic aperture can be increased because small-scale asperities along the surface will not perfectly match. Thus, the fracture may remain partially open (Mayerhofer et al 1997).

Weng et al. (2015) believe that low-viscosity fluids are more favorable in inducing shear-slip because high-viscosities will reduce the distance of fluid penetration. Finally, it is important to remember that shear reactivation of the natural fractures is an important cultural factor because it is one of the major causes of small or even large-scale seismic events (Warpinski et al 1987, , Holland 2013, Maxwell et al 2015).

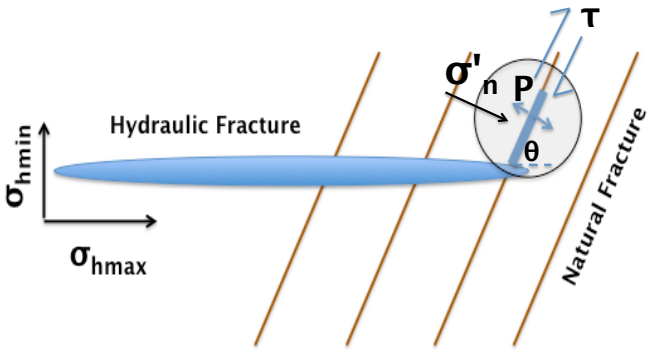

Fig. 2. Shear reactivation of natural fracture caused by pore pressure (Modified from Weng et al. 2015). The hydraulic fracture hits the natural fracture. Natural fracture dilates due to low effective normal stress and it creates aperture and hydraulic conductivity.

In recent years, numerous theoretical, numerical and experimental studies have investigated the effect of variable roughness geometries and loading conditions on asperity degradation and fluid flow through fractures (Patton, 1966, Ladanyi & Archambault, 1970, Barton, 1973, Plesha 1987, Saeb & Amadei 1992, Gentier et al., 2000, Grasselli & Egger 2003). Although in situ rock fractures are subject to both normal and shear loading (Ishida et al 2010, Moradian et al 2013, Gravel et al. 2015), many previous laboratory investigations have considered only normal stress effects on the aperture and hydraulic conductivity, and only a few researchers have investigated the effect of shear displacement on fluid flow (Olsson and Brown, 1993, Gentier et al. 1997, Yeo et al 1998, Chen et al 2000 and Sharifzadeh et al 2008).

The mechanisms and processes during fault activation resulting in earthquakes, and sliding along rock slopes and in other engineering applications have been widely investigated (Mogi 1962, Brace & Byerlee 1966, Scholz 2002, Moradian et al. 2010, McLaskey et al 2014), but the mechanisms of shear reactivation of natural fractures during hydraulic fracturing has not been fully studied yet. Despite much recent work, a complete understanding of the relationship between natural fracture geometry, applied stresses and aperture has yet to be achieved.

In this work, direct shear loading at constant normal loads (CNL) was conducted on artificial surfaces cast from natural granite joints. The effective normal stresses were relatively small, in order to simulate the second shear-reactivation mechanism discussed above. Our calculations used 3D coordinates of the surface asperities measured using a laser profilometer, to predict the normal and shear displacements and the size and distribution of mechanical apertures along the fracture during shear reactivation.

2. FRACTURE SURFACE PREPARATION AND ROUGHNESS MEASUREMENT

We consider changes in mechanical aperture for a rough joint slipping under low effective-normal stress. Rectangular-shaped joint replicas, 140×140 mm^2, were prepared by pouring non-shrinking cement mortar on a fresh joint surface of an artificially split granite block (Moradian et al. 2012). We assumed that upper and lower surfaces were completely matched at the initial stage of shearing. Thus, the initial aperture and contact area were assumed to be 100% and 0% respectively. The details of the experimental methodology can be found in Fathi et al, 2015 and 2016.

The upper and lower surfaces of the joint replica were scanned by a profilometer before the test. Each surface was approximated by considering a large number of planar surfaces tangent to the asperities at a given point

(Fathi *et al*. 2015). Each of these tiny windows could be characterized by their heights above a reference plane and their angle of inclination with respect to the coordinate system. Each asperity was characterized by several tiny windows. The frequency distribution and a map view of tiny windows as a function of their heights and angles are shown in Figures 3 and 4 respectively.

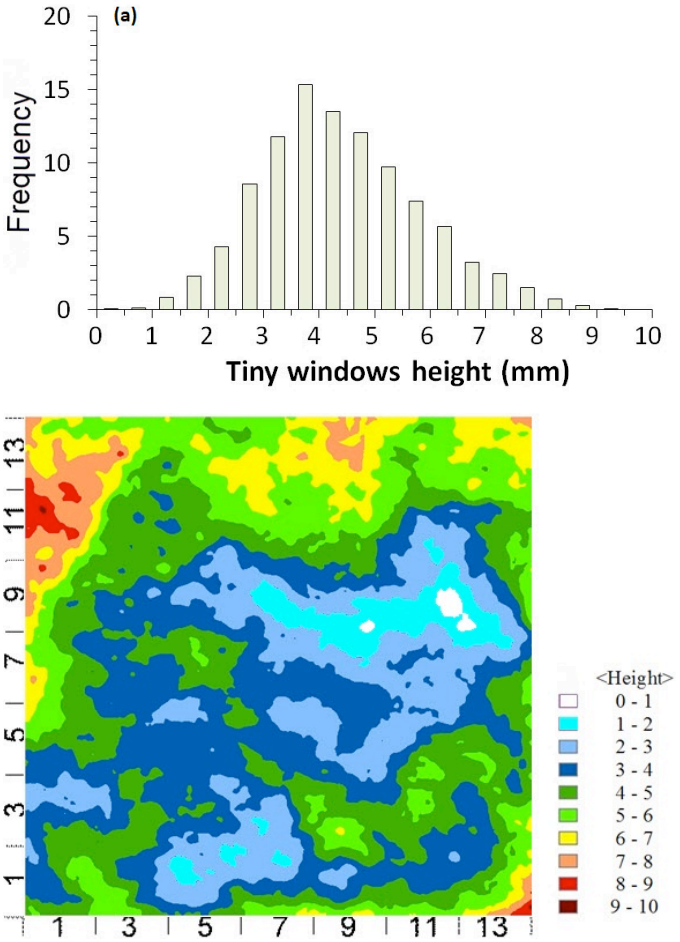

Fig. 3. a) Frequency distribution and b) map view of tiny windows of the fracture surface as a function of their heights.

Almost half of the tiny windows (49%) have a negative angle with respect to the shear direction (white zones in Figure 4b). During the initial sliding, when windows along the upper surface have negative angles, those points do not sustain normal loads after a slip increment. Dilation occurs at that point, increasing the mechanical aperture (see Figure 5). Asperities with windows that have positive angles (colored zones) interfere with the opposing substrate, hinder sliding, and are locations where damage can occur.

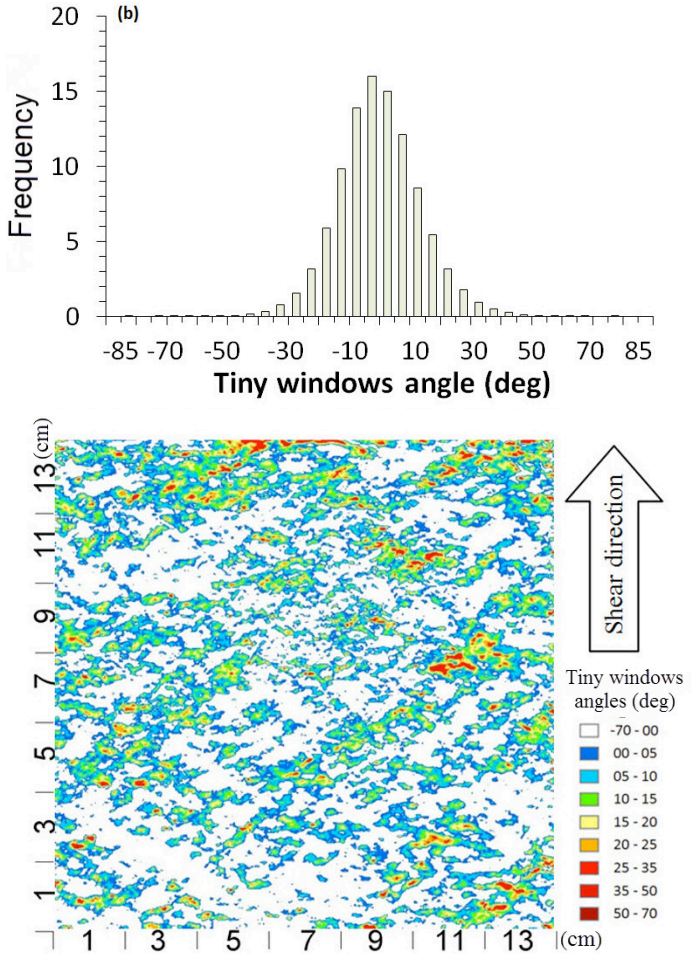

Fig. 4. a) Frequency distribution and b) map view of tiny windows of the fracture surface as a function of their angles. The colored and white zones show tiny windows with positive and negative angles toward the shear direction respectively

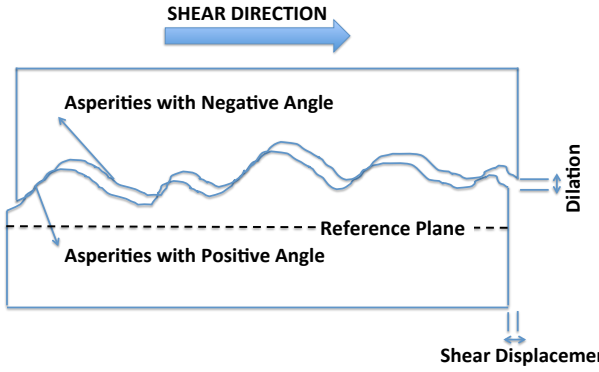

Fig. 5. Asperities with positive and negative angles toward the shear direction. Asperities with negative angles open right after slip initiation while asperities with positive angle may open later according to their heights and the amount of dilation.

3. MECHANICAL APERTURE CALCULATION

Assuming laminar flow between two smooth parallel plates, then hydraulic conductivity of the fracture is given by the cubic law (Zimmerman and Bodvarsson 1996):

$$k = ge^2 / 12v$$

where k = hydraulic conductivity, g = gravity acceleration, e = hydraulic aperture averaged over the entire joint and v = viscosity of the fluid. This assumption is a substantial simplification: The surfaces formed during hydraulic fracturing are not smooth; and the asperities along them have important consequences on fluid flow. The most evident effect is that the flow surfaces lose their parallelism; moreover, in comparison with a smooth joint with equal aperture, a rough joint can cause changes in both the local aperture and the flow path. It is possible that all these factors can actually reduce hydraulic conductivity in the reservoir (Scesi & Gattinoni 2009). To consider these effects, the real aperture between two surfaces must be calculated by taking into account the effect of surface roughness. A first estimation can be obtained by taking the mean mechanical aperture as a measure of void spaces existing between fracture surfaces.

Barton et al. (1985) proposed that the effect of roughness on hydraulic aperture could be included by using the following empirical relation:

$$e = (JRC)^{2.5}(E/e)^{-2}$$

where e is hydraulic aperture (μm), E is mechanical aperture (μm) and JRC is joint roughness coefficient.

The techniques used to measure mechanical aperture include injection, X-ray Computer Tomography (CT), Nuclear Magnetic Resonance Imaging (NMRI), gas volume balance, laser scanner and photogrammetry (Hakami 1995, Chen et al 2000, Sharifzadeh et al 2008). In this study, we used a profilometer to scan the 3D coordinates of the joint surfaces. Since the upper surface has been casted by pouring cement on the lower surface, we assumed that the two surfaces were initially fully mated, that the initial contact area was 100%, and therefore, that the initial aperture would be 0%. In this case, during the scanning, common reference points must established to match the opposing surfaces (Fathi et al 2015). If the two surfaces were not completely mated, then the initial aperture would need to be measured using displacement vectors at each of the reference points.

During the shear experiment, the lower surface is fixed and the upper one slides over it. After each increment of shear displacement, we calculated new 3D coordinates for each of the tiny windows of the upper surface using the measured shear and normal displacements. The coordinate system is selected so that x-axis is along the shear direction, the y-axis is perpendicular and contained within the reference plane, and the z-axis gives the asperity height.

$$X_{iup} = x_{iup} + dx$$
$$Y_{iup} = y_{iup}$$
$$Z_{iup} = z_{iup} + dz$$

where dx is shear displacement, dz is normal displacement and, $x_{iup}, y_{iup}, z_{iup}$ and $X_{iup}, Y_{iup}, Z_{iup}$ are the initial and the new coordinates of the i^{th} point on the upper (mobile) surface respectively.The profile of the lower surface was assumed to be rigid and fixed during the test. In other words, the lower surface does not damage or displace, neither normally nor tangentially, as a function of shear and normal displacements and all the damage and displacement occurs in the upper surface.

We assume that there is no rigid body rotation or lateral movement of either surface around or along the y-axis; thus the y coordinates of points on either the upper or lower surfaces do not change during the test. We also assumed that shear and normal loads/displacements were applied uniformly on the entire surface of the joints. Thus, if there is 1mm shear or normal displacement, all asperities displace 1 mm normally or tangentially. After slip, the difference of the heights of the windows on the upper and lower faces determines whether the two tiny windows at a given x,y position are still in contact.

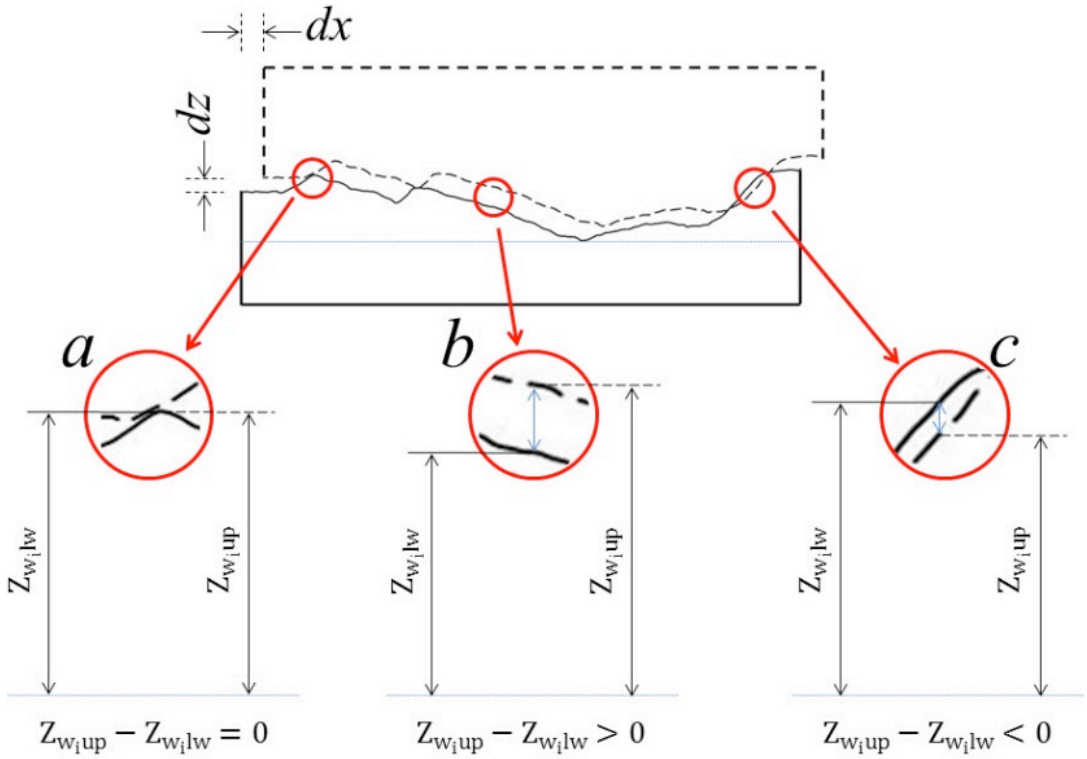

Fig. 6. Assessment criteria for mechanical aperture calculation; a) zero aperture= tiny windows are just in-contact, b) positive aperture= tiny windows are not in contact c) negative aperture= damaged has occurred and gouge materials have been produced (Fathi et al 2015)

We did not consider elastic deformation in the shear plane, but we did include elastic distortions in the normal direction. Based on tensile tests on cylindrical specimens the maximum elastic displacement for the specimens was 0.01 mm. After taking into account the elastic deformation, the criteria for mechanical aperture calculation are as follows:

- if $Z_{w_i up} - Z_{w_i lw} < 0$ tiny windows have been damaged, negative aperture
- if $0 < Z_{w_i up} - Z_{w_i lw} < 0$ Tiny windows are just in contact, zero aperture
- if $0 < Z_{w_i up} - Z_{w_i lw}$ Tiny windows are not in contact, positive aperture

where $Z_{w_i up}$ and $Z_{w_i lw}$ are the height of the i^{th} tiny window of the upper and lower surfaces (Figure 6).

We considered negative apertures to be zones where damage occurred and that the volume of debris formed in the damage zones would fill the regions with positive aperture. As a result, the total volume of mechanical aperture available for fluid flow is the subtraction of the negative apertures from the positive apertures:

$$\text{Total volume of mechanical aperture} = \sum A \times (\Delta z_i > 0) - \sum A \times (\Delta z_i < 0) = A \times \sum (\Delta z_i > 0 - \Delta z_i < 0)$$

Where A is the area of a tiny window (0.2×0.2 mm^2), $\Delta z_i > 0$ are positive apertures and $\Delta z_i < 0$ are negative apertures.

4. MECHANICAL APERTURE DISTRIBUTION DURING DIRECT SHEAR TEST

We measured the force necessary to cause sliding during direct shear test for several normal loads, and the actual shear and normal displacements between the two joint surfaces during slip. Dilation is the increase in the relative normal displacement between the upper and lower surfaces. The shear displacement rate was 0.1 mm/min; the tests were ended when the shear displacement attained 10 mm (Moradian 2010). Figure 7 displays the direct shear test results for the tested specimens.

We note that dilation monotonically increases up to 10 mm. This result probably owes to the fact that the shear displacement would need to overpass the asperity with highest wavelength before dilation would decrease. The highest wavelength in the roughness distribution is about 22 mm, which is larger than the maximum shear displacement (10mm). After the slip distance surpasses the highest wavelength, dilation could decrease. But, because the surfaces have random distributions of asperity height, it is unlikely that dilation would go to zero, unless gouge production is large. In this study, we considered the case where both the applied normal stresses and the amount of gouge materials were low. Nevertheless, at higher shear displacements where the contact area is reduced due to dilation, even this low initial normal stress produces very high stress concentrations and some gouge materials may be

produced. For these calculations, the positive effect of dilation overcomes the negative effect of gouge production, and therefore, aperture increases. Figure 8 shows the local shear stress as a function of shear displacement for given normal loads using the actual contact area calculated from the tiny window method.

In contrast, if normal stresses were higher, dilation might be less significant, and gouge production could play a dominant role in changing the aperture and hydraulic conductivity (Barton and Quadros 1997). Using the methodology in section 3, the mechanical aperture of the joint surfaces under different normal loads and after each shear displacement increments was calculated from the shear and normal displacements of the two surfaces.

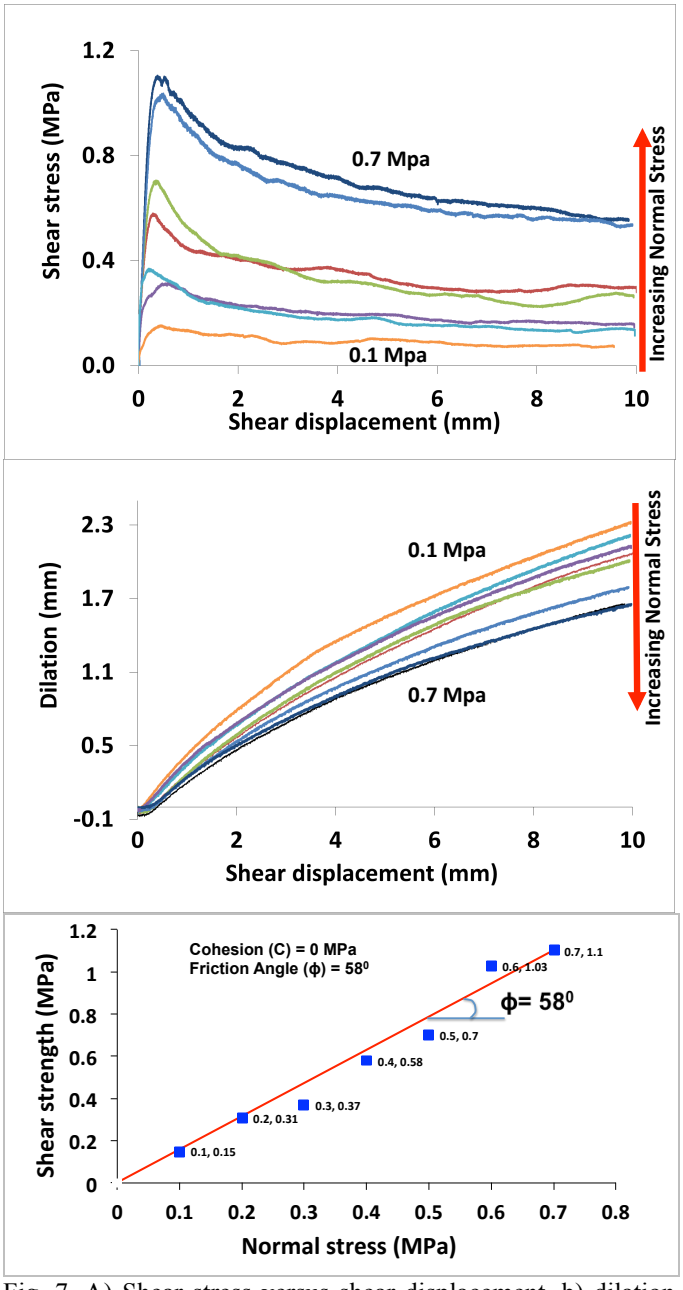

Fig. 7. A) Shear stress versus shear displacement, b) dilation versus shear displacement and c) cohesion and maximum friction angle of the tested specimens

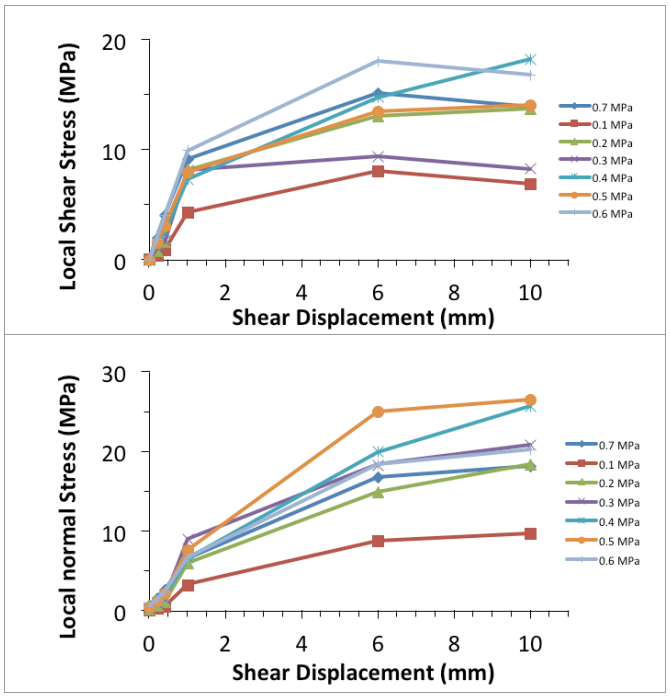

Fig. 8. The local shear and normal stresses applied after different shear displacements. At each shear displacement the real contact area has been calculated and the shear and normal stresses have been calculated based on that contact area rather than the whole area between the joint surface.

Figure 9 displays the frequency and distribution of the tiny windows as well as their aperture after slip displacements of 0.2, 0.4, 1, 6 and 10 mm.

As can be seen in Fig. 9, mechanical aperture (white color zones) starts increasing as shear displacement begins. From Figure 9c, it can be inferred that a shear displacement as low as 1 mm is enough to increase mechanical aperture to 2 mm and the volumetric aperture up to 90%. Further shear displacements (e.g. 6 mm or 10 mm) increase the mechanical aperture up to 3.5 mm and the volumetric aperture up to 99%.

Figure 10 and 11 show the change in mechanical aperture as a function of normal stress and slip displacement. While aperture is reduced by increasing normal stress, it is increased significantly by slip displacement.

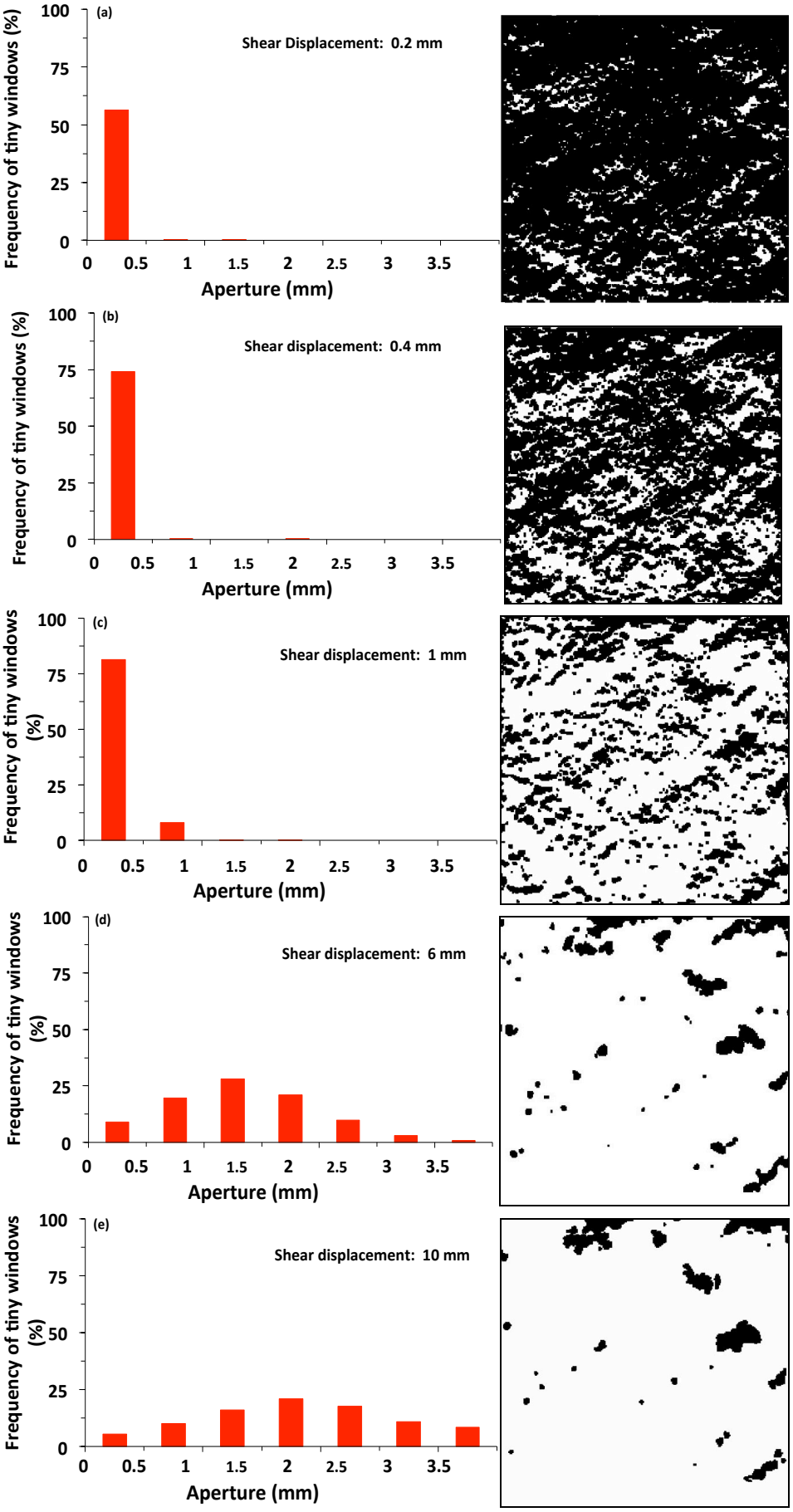

Fig. 9. a) Frequency of tiny windows vs their mechanical aperture and b) map of mechanical aperture distribution after 0.2, 0.4, 1, 6 and 10 mm shear displacement under 0.7 MPa normal stress. Black and white colors show in-contact and open (aperture) zones respectively.

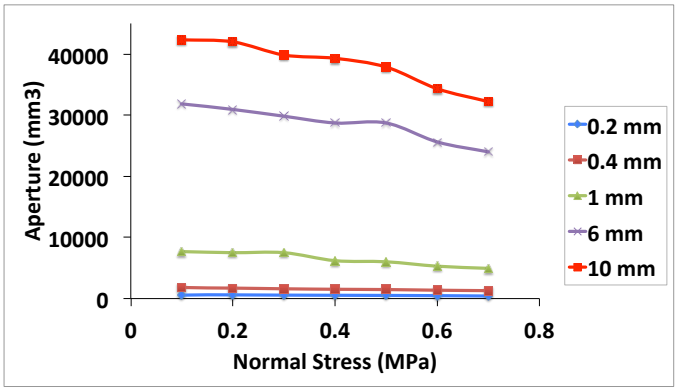

Fig. 10. Total Volume of mechanical aperture as a function of normal stress for various shear displacements. Since the initial aperture is 0%, changing in normal stress wouldn't affect the aperture though some elastic closing (interlocking of upper and lower asperities) may happen in high normal stresses.

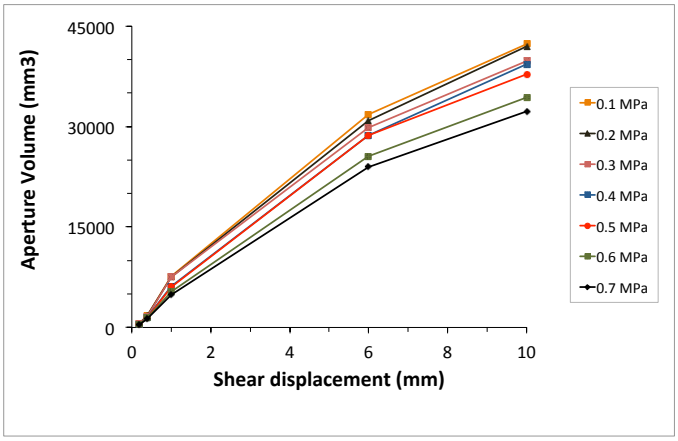

Fig. 11. Total Volume of mechanical aperture as a function of shear displacement for various normal stresses. By increasing shear displacement the effect of initial normal stress on the aperture will be more pronounced.

5. DISCUSSION

While the results have shown that the shear reactivation of natural fractures increases the aperture of the natural fracture, the following conditions are important in determining the changes in the transmissivity of the un-propped natural fractures:

I. The hydraulic fracture must intersect the natural fracture so that the hydraulic fracturing fluid can be exchanged.
II. The natural fracture must be permeable so that the fluid can penetrate a significant distance into the natural fracture.
III. Matrix permeability must be low compared to fracture transmissivity. If matrix permeability is high, natural fractures will have a small effect on the fluid transmisivity (Weng et al 2015).
IV. Pore pressure must be close to σ_{hmin}, so that effective normal stress is reduced close to or even below zero. This is because the natural fractures are too strong to slip as the hydraulic fracture approaches, but they begin to fail as the fracturing fluid enters and decreases the effective normal stress (Maxwell et al 2015).
V. The azimuth/orientation of the natural fracture must be at an angle with respect to the *in situ* principal stresses that is sufficient to produce a substantial shear stress resolved on the slip plane. Similarly, larger stress anisotropy is more favorable in inducing shear slip propagation (Weng et al 2015).
VI. These experiments and calculations considered rigid sliding of fractures where shear damage is relatively small. In this case, primarily where normal loads are small, dilation happens, aperture is produced and the amount of gouge materials is not significant. Under higher effective normal loads, aperture and hydraulic conductivity may not change significantly because of the competing effects of fracture dilation and gouge formation. Because gouge production systematically reduces hydraulic conductivity, considerations of this case will demand a change in viewpoint from that of parallel plate or channel flow to flow in porous medium with changing microstructure (Barton and Quadros 1997).
VII. Shear slippage of the natural fracture must not exceed a certain amount (shear slippage < highest asperity wavelength and shear slippage<opening of the hydraulic fracture), because:
   A. If we overpass the highest asperity wavelength, the dilation decreases and the natural fracture may close.
   B. Since shear-slip makes a relative shift of the joint surfaces on two sides of the natural fracture, it forms a small offset in the main hydraulic fracture. It is therefore possible that too much shear-slip can cause a shift exceeding the fracture width, cutting off the main hydraulic fracture at the natural fracture junction (Weng et al 2015).

6. CONCLUSIONS

A methodology was proposed for calculation of volumetric mechanical aperture of two joint surfaces under different, but low, normal loads and slip distances. The calculations suggested that shear reactivation of natural fractures during a proppant-free hydraulic fracturing operation can significantly enhance mechanical aperture, which eventually leads in an enhancement in hydraulic aperture and conductivity.

One of the interesting topics considered in these calculations are the competing effects of dilation and gouge production. Under low effective normal stress, natural fractures dilate more than damage, and therefore aperture increases.

Under these conditions, the slip distance affects

mechanical aperture more than the effect of normal stress. Shear displacements as low as 1 mm are enough to increase the mechanical aperture (≈ 90%) up to 2 mm. Further shear slip (e.g. 6 mm or 10 mm) increases the aperture volume by about 98% and the aperture up to 3.5 mm.

7. ACKNOWLEDGMENTS

The authors would like to thank TOTAL SA for supporting this research. The collaboration of the Civil Engineering Department at Sherbrooke University is greatly acknowledged for test results.

REFERENCES

1. Amadei, B. and Illangasekare, T., Analytical solutions for steady and transient flow in non-homogeneous and anisotropic rock joints. Int. J. Rock Mech. Min. Sci. Geomech. Abstr., 1992, PWD 561-572.
2. Barton N, Bandis S, Bakhtar K. Strength, deformation and conductivity coupling of rock joints. Int J Rock Mech Min Sci Geomech Abstr 1985;22(3):121–40.
3. Barton N, Quadros EF. Joint aperture and roughness in the prediction of flow and groutability of rock masses. In: Kim K, editor. Proceedings of the NY Rocks'97. 'Linking Science to Rock Engineering. Int J Rock Mech Mining Sci 1997;34(3–4): 907–16.
4. Barton, N. (1973) Review of a new shear strength criterion for rock joints, Quarterly Journal of Engineering Geology, 7, p. 287–332.
5. Brace WF, Byerlee JD (1966). Stick-slip as a mechanism for earthquakes. Science 153:990–992
6. Cipolla, C.L., Lolon, E.P., Mayerhofer, M.J., and Warpinski, N.R. 2009. The Effect of Proppant Distributionand Un-Propped Fracture Conductivity on Well Performance in Unconventional GasReservoirs. Paper SPE 119368 presented at the SPE Hydraulic FracturingTechnology Conference, The Woodlands, Texas, USA, 19-21 January. doi:10.2118/119368-MS.
7. Chen Z, Narayan SP, Yang Z, Rahman SS. An experimental investigation of hydraulic behaviours of fractures and joints in granitic rock. International Journal of Rock Mechanics and Mining Sciences 2000; 37:1061–1071.
8. Fathi A., Moradian Z., Rivard P., Ballivy G., Boyd A. (2015). Geometric Effect of Asperities on Shear Mechanism of Rock Joints. Rock Mechanics and Rock Engineering Journal. DOI 10.1007/s00603-015-0799-6.
9. Fathi A., Moradian Z., Rivard P., Ballivy G (2016). Shear Mechanism of Rock Joints Under Pre-peak Cyclic Loading Condition. International Journal of Rock Mechanics and Mining Sciences. Volume 83, Pages 197–210.
10. Gentier, S., Lamontagne, E., Archambault, G. and Riss, J., Anisotropy of flow in a fracture undergoing shear and its relationship to the direction of shearing and injection pressure. Int. J. Rock Mech. Min. Sci. Geomech. Abstr.(Paper No. 094), 1997, QRD 3-4.
11. Gentier, S., Riss, J., Archambault, G., Flamand, R., Hopkins,D. (2000), Influence of fracture geometry on shear behavior. Int. J. Rock. Mech. Min. Sci. & Geomech. Abstr. 37(1–2) , p. 161–174.
12. Grasselli, G., and Egger, P. (2003). "Constitutive law for the shear strength of rock joints based on three-dimensional surface parameters." Int. J. Rock Mech. Min. Sci., 40(1), 25-40.
13. Gravel, C. Moradian, Z. Fathi, A. Ballivy G.and Rivard, P. (2015). In situ shear testing of simulated dam concrete-rock interfaces. ISRM 2015. May 10-15, Montreal, Canada
14. Hakami, E., Aperture distribution of rock fractures. Ph.D. the- sis, Royal Institute of Technology, Stockholm, Sweden, 1995.
15. Holland, A. Earthquakes triggered by hydraulic fracturing in south-central Oklahoma. Bull. Seismol. Soc. Am. 103, 1784–1792 (2013).
16. Ishida T, Tadashi Kanagawa, Yuji Kanaori. (2010), Source distribution of acoustic emissions during an in-situ direct shear test: Implications for an analog model of seismogenic faulting in an inhomogeneous rock mass. Engineering Geology: 110(3-4), p. 66-76.
17. Jansen T., Zhu D., Hill A. D., 2015. Effect of Rock mechanical properties on fracture conductivity for shale formations, SPE 173347-MS HFTC, Woodlands, TX, 3-5 Feb.
18. Ladanyi, B., Archambault, G. (1970), Simulation of shear behavior of a jointed rock mass. 11th Symposium on Rock Mechanics, Berkeley, p. 105–125.
19. Maxwell, S. C., Mack, M., Zhang, D. et al. 2015. Differentiating Wet and Dry Microseismic Events Induced During Hydraulic Fracturing. Presented at the Unconventional Resources Technology Conference, San Antonio, Texas, USA, 20–22 July. URTeC 2154344.
20. Mayerhofer, M. J., Richardson, M. F., Walker, Jr., R. N., Meehan, D. N., Oehler, M. W., and Browning, Jr., R. R., 1997, Proppants? We don't need no proppants: Proc. 1997 Soc. Petr. Eng. Ann. Tech. Conf., Paper 38611.
21. McLaskey, G. C., B. D. Kilgore, D. A. Lockner, and N. M. Beeler (2014), Laboratory generated M 6 earthquakes, Pure Appl. Geophys., doi:10.1007/s00024-013-0772-9.
22. Mogi, K. (1962). Magnitude-frequency relation for elastic shocks accompanying fractures of varios materials and some related problems in earthquakes, Bull. Earthq. Res. Inst. 40, 831–853.

23. Moradian, Z. A, G. Ballivy, P. Rivard, C. Gravel and B. Rousseau (2010a). Evaluating damage during shear tests of rock joints using acoustic emission. International Journal of Rock Mechanics and Mining Sciences, Vol. 47, No. 4, pp 590–598.

24. Moradian, Z. A, G. Ballivy, P. Rivard, (2012a). Application of acoustic emission for monitoring shear behavior of bonded concrete-rock joints. Canadian Journal of Civil Engineering, Vol. 39, pp 887-896.

25. Moradian, Z. A, G. Ballivy, P. Rivard, (2012b). Correlation acoustic emission source locations with damage zones of rock joints under direct shear test. Canadian Geotechnical Journal, Vol. 49, No. 6, pp 710-718

26. Moradian, Z. Gravel, C. Fathi, A. Ballivy, G. Rivard, P. Quirion, M. (2013). Developing a high capacity direct shear apparatus for large scale laboratory testing of rock joints. ISRM International Symposium EUROCK 2013, September 21-26, Wroclaw, Poland.

27. Patton, F.D. (1966) Multiple modes of shear failure in rocks, Proceedings of First Congress of International Society of Rock Mechanics, Portugal, Vol.1, p. 509–513.

28. Plesha ME. Constitutive models for rock discontinuities with dilatancy and surface degradation. Int J Numer Anal Meth Geomech 1987;11:345–62.

29. Saeb S, Amadei B. Modelling rock joints under shear and normal loading. Int J Rock Mech Min Sci Geomech Abstr 1992;29: 267–78.

30. Scesi, L., P Gattinoni, 2009, Water Circulation in Rocks, Springer , DOI 10.1007/978-90-481-2417-6

31. Scholz, C. H., 2002, The mechanics of earthquakes and faulting: Cambridge, Cambridge University Press, second edition.

32. Sharifzadeh M, Mitani Y, Esaki T. Rock joint surfaces measurement analysis of aperture distribution under different normal, shear loading using GIS. Rock Mech Rock Eng 2008;41:299–323.

33. Warpinski, N.R., and Teufel, L.W., 1987. Influence of Geologic Discontinuities on Hydraulic Fracture Propagation (includes associated papers 17011 and 17074). SPE Journal of Petroleum Technology 39(2): 209-220.

34. Weng, X., Sesetty, V., Kresse, O., (2015) Investigation of Shear-Induced Permeability in Unconven- tional Reservoirs. 49th US Rock Mechanics / Geomechanics Symposium held in San Francisco, CA, USA, 28 June-1 July 2015.

35. Yeo IW, de Freitas MH, Zimmerman RW. Effect of shear displacement on the aperture and permeability of a rock fracture. Int J Rock Mech Min Sci 1998; 35(8):1051–70.

36. Zhang J., Kamenov A., Zhu D., Hill A. D., 2013. Laboratory measurement of hydraulic fracture conductivities in the Barnett shale, SPE 163839 SPE HFTC, Woodlands, TX, 4-6 Feb.

37. Zimmerman, R. W. and Bodvarsson, G. S., Hydraulic conductivity of rock fractures. Transport Porous Media, 1996, PQD 1-30.

38. Zoback, M.D., A. Kohli, K. Das, and M. McClure. 2012. The Importance of Slow Slip on Faults During Hydraulic Frac- turing Stimulation of Shale Gas Reservoirs. Richardson, Texas: SPE 155475.